IEEE Photonics Journal
An IEEE Photonics Society Publication

Open Access

An Injection-Locked Single-Longitudinal-Mode Fiber Ring Laser With Cylindrical Vector Beam Emission

Volume 9, Number 1, February 2017

Hongdan Wan
Hongye Li
Changle Wang
Bing Sun
Zuxing Zhang
Wei Wei
Lin Zhang

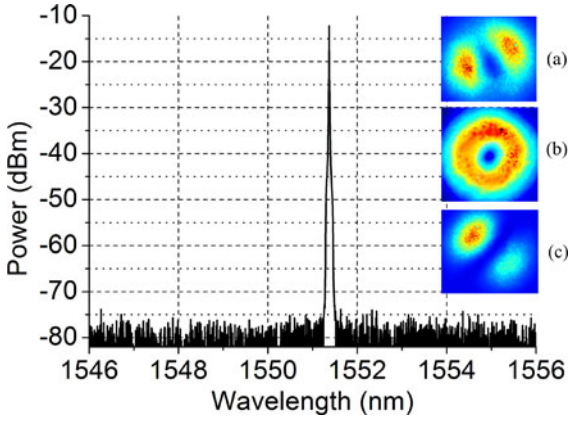

DOI: 10.1109/JPHOT.2017.2653618
1943-0655

IEEE photonics SOCIETY

IEEE

An Injection-Locked Single-Longitudinal-Mode Fiber Ring Laser With Cylindrical Vector Beam Emission

Hongdan Wan,[1] Hongye Li,[1] Changle Wang,[2] Bing Sun,[1] Zuxing Zhang,[1,2] Wei Wei,[1] and Lin Zhang[1,2]

[1]Nanjing University of Posts and Telecommunications, Nanjing 210023, China
[2]Aston Institute of Photonic Technologies, Aston University, Birmingham B4 7ET, U.K.

DOI:10.1109/JPHOT.2017.2653618

Manuscript received December 1, 2016; revised January 5, 2017; accepted January 9, 2017. Date of publication January 16, 2017; date of current version February 7, 2017. This work was supported in part by the National Science Foundation of Jiangsu Province (Nos. BK20150858 and BK20161521), in part by the NUPTSF (Nos. NY214059 and NY213083), in part by the Distinguished Professor Project of Jiangsu (No. RK002STP14001), in part by the Six Talent Peaks Project in Jiangsu Province (No. 2015-XCL-023), and in part by the Talents Projects in Nanjing University of Posts and Telecommunications (Nos. NY214002 and NY215002). Corresponding authors: H. Wan and Z. Zhang (e-mail: hdwan@njupt.edu.cn; zxzhang@njupt.edu.cn).

Abstract: We demonstrate a fiber ring laser with narrow bandwidth single-longitudinal-mode cylindrical vector beam (CVB) output at C-band wavelength range for the first time to the best of our knowledge. A step index two-mode fiber Bragg grating is used as a transverse mode selector for CVB generation, while both the injection-locking technique and narrow bandwidth of the fiber Bragg grating lead to single-longitudinal-mode operation. The 3-dB bandwidth of the laser output is measured to be $<$0.01 nm near a single wavelength of 1551.4 nm with a signal-to-background ratio of $>$60 dB. Mode distribution and optical spectra of few-mode fibers with periodic modulated refractive index profile, namely the few-mode fiber Bragg gratings with bent radius, are investigated theoretically and experimentally, which provide a comprehensive exploration of CVB's generation.

Index Terms: Fiber laser, fiber gratings, optical fiber devices.

1. Introduction

Cylindrical vector beam (CVB) generation has drawn considerable attention recently for its symmetric intensity and polarization properties. The symmetrical polarization light beams are desirable for many applications, such as optical tweezers, surface plasmon resonance and material processing [1]–[4]. Various "passive" (extra-cavity) and "active" (intra-cavity) methods are used to generate CVBs [5]—[16], such as the birefringence elements [6], spatial light modulators [7], sub-wavelength gratings [8], and few-mode fiber gratings [9]–[13], fiber grating with periodic microbends [14]. Compared with free-space mode selectors, all-fiber polarization-selective elements such as fiber gratings have the advantages of high efficiency, high compactness, and flexibility. The fiber Bragg grating (FBG) in single-mode fiber can be a usual wavelength selector for fiber lasers [17], [18], while few-mode fibers (FMFs) with relatively larger core diameter can sustain more than one transverse mode. Correspondingly, the FBG in FMF offers more than one Bragg wavelength.

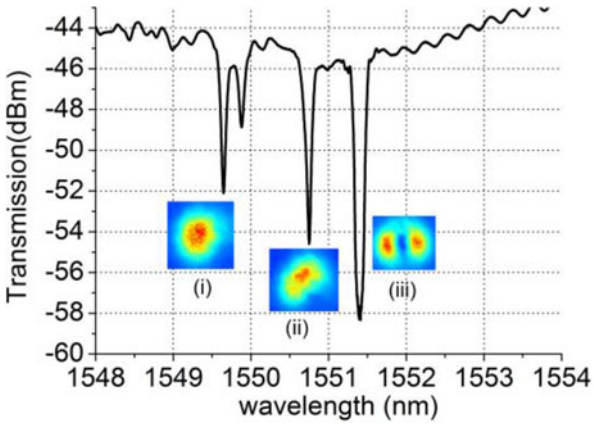

Fig. 1. Measured transmission spectrum of the step-index two-mode FBG. (Inset) Modal profiles near the three different transmission-dip wavelengths measured by CCD.

Recently, various "active methods" for pulsed CVB generation have been reported based on mode-locking and Q-switching method inside a fiber cavity, using FM-FBGs as the transverse mode selector. Yan and Lin reported a passively Q-switched fiber laser with CVB output using a Bi_2Te_3 as the saturable absorber in a ring cavity [9]. Sun *et al.* achieved mode-locked radially polarized rectangular pulses within a Fig. 8 cavity and actively mode-locked CVB pulses using a $LiNbO_3$ Mach–Zehnder modulator and a step index four-mode FBG within a ring cavity [10], [11]. They also demonstrated a fiber laser generating CW CVB within a linear cavity having a switchable wavelength near 1050 nm [12], [13].

Narrow bandwidth, single-longitudinal-mode (SLM) laser operation with good stability, low noise and high coherence is important for many optical communication and sensing systems. However, to the best of our knowledge, until now there is no report about narrow bandwidth, SLM all-fiber laser with CW CVB output at C-band wavelength range. On the other hand, the case of step index FM-FBG with uniform refractive index profile over round fiber core has been discussed in previous work. However, it is difficult to fabricate perfectly round core in high NA fibers and UV-side-writing grating structure to the core, and bending effect of step index few mode fiber would result in non-uniform refractive index profile over the fiber core. Therefore, optical properties of a step index FM-FBG with non-uniform refractive index profile have to be considered for CVB generation.

In this paper, we present a SLM fiber laser at C-band wavelength based on an injection-locked ring cavity for generating CW CVB using a two-mode FBG as the intracavity transverse mode selector. Modal property and transmission spectra of the step index FM fibers and FM-FBGs with different bent radius are investigated experimentally and theoretically. Our proposed method has the merits of simple structure and high CVB purity and narrow bandwidth.

2. Experimental Results and Discussions

2.1 Optical Property of Step Index Two-Mode FBG

In our experiment, two mode (#60816, with normalized frequency $V = 4.6$) step index fibers from OFS ltd is used for FBG inscription. The hydrogenation process for both kinds of fibers is always necessary before grating inscription, due to their low photosensitivity. During this process, fibers are treated in 150-bar pressure H_2 chamber at 80 °C temperature for 60 hours. We use phase mask scanning method to fabricate FBGs using a 244 nm Argon-ion frequency-doubled laser. The period of the phase mask is 1071.92 nm, so the grating period is 535.96 nm.

Fig. 1 shows the transmission spectrum of the step-index two-mode FBG, measured by an optical spectrum analyzer (OSA) with a resolution bandwidth of 0.01 nm. During the splicing of single

TABLE 1
MODAL PROFILE OF THE STEP-INDEX TWO-MODE FIBER WITH DIFFERENT BENT RADIUS *r*

Mode	Bent Radius (cm) ∞	10	5	2	1
LP01	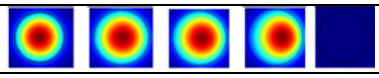				
LP11	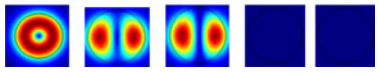				

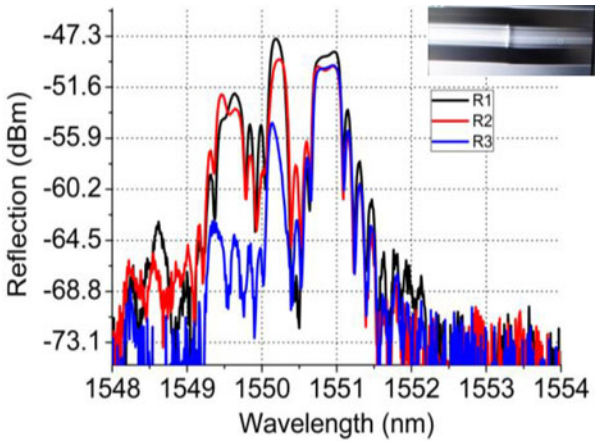

Fig. 2. Measured reflection spectra of the step index two-mode FBG with different bent radius *R*. High order mode is excited with a LOS of 4 μm; the decreased *R* results in reduced reflection peak power of self-coupling.

mode fiber (SMF) and two-mode fiber, we introduced a lateral offset splicing (LOS) of 3–4 μm between the endfaces of the two fibers to excite the high-order mode. The modal profiles near three transmission-dip wavelengths are shown in the inset figures (measured by a CCD, CinCam IR).

Three kinds of mode-coupling process are involved, namely (i) the self-coupling of the LP11 mode (1549.7 nm); (ii) the mutual-coupling between the LP11 and LP01 mode (1550. 9 nm); and (iii) the self-coupling of the LP01 mode (1551.4 nm). In the inset figure (iii), the LP01 mode is reflected and the LP11 mode transmits through the FBG near 1551.4 nm and is detected by the CCD. However, the pressure and bending effect introduced by a fiber holder result in a non-uniform refractive index profile over the fiber core, the modal profile of LP11 mode takes on an asymmetric two-lobe shape, which is in good accordance with our simulations (see Table 1).

To further explore the bending effect on the reflection spectrum of the step index two-mode FBG, we measured reflection spectra of the FBG with different bent radius (the two-mode fiber except the FBG section is coiled; R1>R2>R3), as shown in Fig. 2. LP11 mode is excited through the LOS as shown in the inset of Fig. 2, resulting in several peaks in the two-mode FBG's reflection spectra. It is clear from the figure that smaller bent radius results in lower intensity of LP11 mode. The peak wavelength intensity is weakened most for LP11-LP11 self-coupling (near 1549.7 nm), which agrees well with our following theoretical simulations: higher order modes lose energy faster than lower modes as bent radius decreases, which results in a reduced self-coupling reflection peak power.

2.2 The SLM Injection-Locked CVB Fiber Ring Laser Based on Two-Mode FBG

Then, based on the step index two-mode FBG, a SLM injection-locked CVB fiber ring laser was proposed and demonstrated. The configuration of the fiber laser is shown in Fig. 3. A 980 nm pump

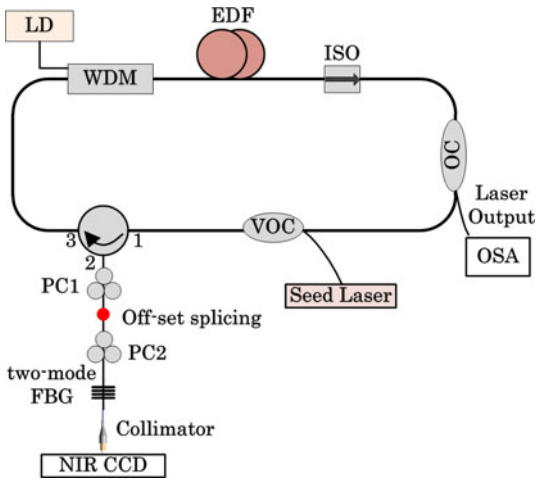

Fig. 3. Configuration of the proposed injection-locked CVB fiber ring laser and the measurement devices. LD: laser diode, EDF: Erbium doped fiber, WDM: wavelength division and multiplexing, VOC: variable optical coupler, PC: polarization controller, ISO: isolator.

LD is coupled to an EDF (Coreactive, EDFL 1500) with a length of 5 m by a WDM. A tunable seed laser with a 3 dB bandwidth of 0.01 nm and a maximum power of 5 dBm is injected into the fiber ring cavity through a VOC (tuning range of coupling 1% $\sim$ 99%). The two-mode FBG is connected to the SMF pigtail of another circulator with a LOS of 6 μm. PC1 and PC2 is used to remove the degeneracy of the second-order modes to obtain TM01, TE01 modes. ISO is used to ensure unidirectional operation. An OC is used to offer feedback and laser output for detection. Before the transmitted light from the two-mode FBG is collimated and measured by the NIR-CCD, the fiber pigtail of the FM-FBG is kept short and straight with minimized bending effect. CVB is generated and detected by the CCD when the fiber ring laser wavelength is injection-locked to the wavelength where the LP01 mode is self-coupled in the two-mode FBG and reflected into the ring cavity. The master (seed) laser forces the slave laser (fiber ring laser) to operate exactly on the injected frequency when the frequencies of the slave laser and the free-running master laser are sufficiently close. Mode competition and noise level of the slave laser is strongly reduced and by sweeping the seed laser's wavelength near the LP01-LP01 self-coupling wavelength with LP01 mode been suppressed.

The SLM laser spectrum is measured as in Fig. 4. The injection-locked CVB fiber laser operates at a single wavelength of 1551.4 nm with a 3 dB bandwidth of less than 0.01 nm and a signal-to-background ratio of more than 60 dB when the injected seed laser has a maximum power of 5 dBm. The laser output power is about 3.8 mW under a pump power of 100 mW. The inset pictures Fig. 4(a)–(c) shows the measured laser beam intensity distribution (modal profile). Cylindrical vector beams are achieved by adjustment of the two fiber polarization controllers carefully. Fig. 4(b) shows the high purity, doughnut shaped modal profile of vector beam captured by the CCD camera. Fig. 4(a) and (c) show the two-lobe-shape intensity distribution profiles.

To validate the laser output is actually a vector beam and investigate modal purity, we measured the CVB intensity distributions after passing through a linear polarizer. The radial and azimuthal polarization of the output mode is confirmed by recording the intensity images by rotating a linear polarizer inserted between the output port and the CCD camera. The results are shown in Fig. 5 with the transmission axis of the polarizer indicated by the white arrows. TE01 and TM01 modes are CVBs, the purity of the azimuthally polarized mode (TE01 mode; see Fig. 5 (b)–(e)) and radially polarized mode (TM01 mode; see Fig. 5 (g)–(j)) are measured and estimated to be 93.1% and 94.6% respectively with the method described in [12] and [13]. CVB with "azimuthal polarization" can be switched to "radial polarization" through carefully adjustment of polarization controllers at two sides of the LOS point. Previous works have proved that the degeneracy of the second-order modes

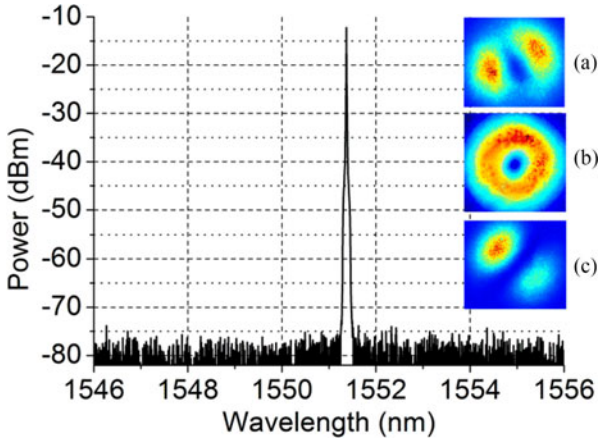

Fig. 4. Injection locked SLM CVB laser output: Optical spectrum of the CVB fiber laser with a 3 dB bandwidth of $<$0.01 nm and a signal-to-background ratio of $>$ 60 dB. (Inset) Laser beam intensity distribution measured at the output port of the collimator with different polarization states.

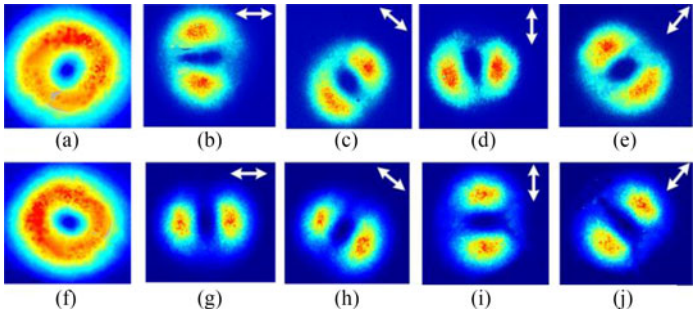

Fig. 5. Intensity distribution of the CVBs with (a) azimuthal polarization (TE01 mode) and (f) radial polarization (TM01 mode). (b)–(e) and (g)–(j) Beam profiles measured after passing through a linear polarizer with the transmission axis orientation denoted by the white arrows.

can be removed by adding polarization controllers to obtain TM01, TE01 modes. The intensity mode profiles of these modes are identical as having a "doughnut" intensity profile. However, as shown in Fig. 5, clear differences can be observed by passing different spatially variant polarization modes through a linear polarization rotated at different orientations.

As to our experimental observations, we achieve single-frequency CVB output when the VOC's intracavity coupling ratio is 1%–20%; however, a larger value will result in un-locked lasing output with mode-hopping appears. Fig. 6 shows the stability measurement of the SLM laser's spectra recorded for two hours at room temperature. During the observing time, no mode-hopping happened, the averaged wavelength variation was less than the OSA's spectral resolution limit and the laser power fluctuation is less than 0.01 dB. The SLM operation is verified by the single sideband RF spectrum as shown in the inset of Fig. 6, measured by a delayed self-homodyne method using a frequency spectrum analyzer (Rohde &Schwarz, FSV30). Based on the injection-locking technique and the FM-FBG, the measured laser oscillation is in a SLM operation [19].

In addition, we compared our method with the "passive method" of putting the same mode convertor (FBG in two-mode fiber) directly after the seed laser without a fiber ring cavity. The resulted optical spectra using the two methods are shown in Fig. 7. It is indicated that, based on transverse mode conversion selection inside a fiber ring cavity, our proposed method has the potential to obtain higher CVB purity, higher power, higher SNR and narrower bandwidth due to the intracavity oscillation process and the injection locking method we used.

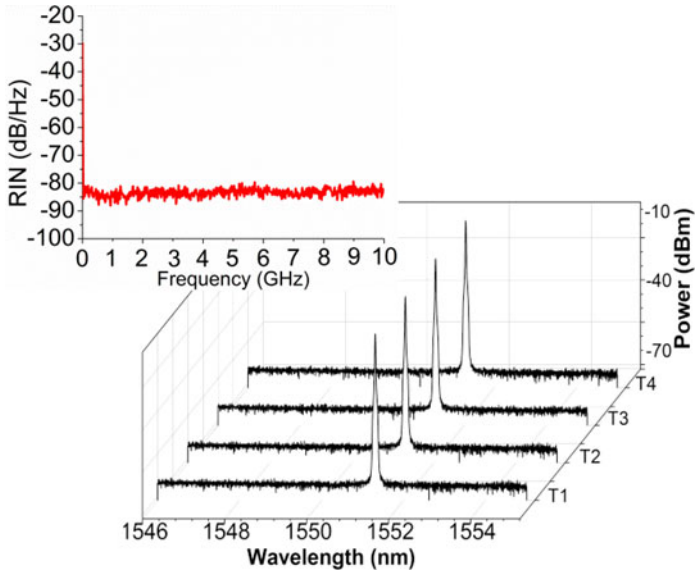

Fig. 6. Mode-hopping-free, SLM lasing spectra measured for two hours. (Inset) Relative noise intensity measured by an RF analyzer.

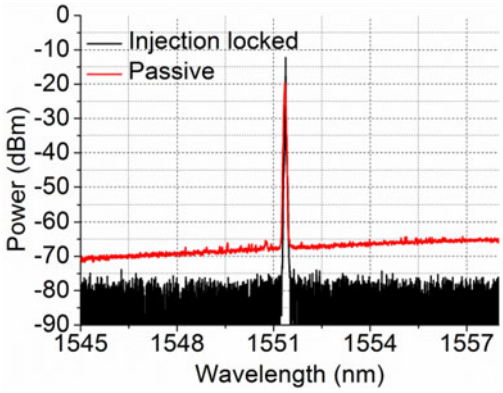

Fig. 7. Comparison of SLM laser spectra generated with the two different methods: Black, our method; Red, passive method.

3. Theory

3.1 Modal Properties of Bent Step Index Two-Mode Fiber

First, we simulated the modal profile of a step index two-mode fiber with different bent radius. The refractive index of bent fiber is described by the Marcuse formula: $n' = n(1 + x/r)$, where n is the refractive index of core, and r is the bent radius. Table 1 shows the electric field amplitude of LP01 and LP11 mode, calculated by finite element method (FEM) for investigation of bending effect on modal intensity distribution in the two-mode fiber.

Actually, the LP11 modes consists of four quasi-degenerate vector modes (HE21 even and odd, TE01, TM01), having ring-shaped intensity profiles with spatially varying polarizations. In our simulated bent fiber core with ellipticity, the electric field amplitude of LP11 mode shows an asymmetric two-lobe-shape distribution, as shown in Table 1. By decreasing the bent radius, LP11 mode dissipates prior to LP01 mode, which is in accordance with the experimental results.

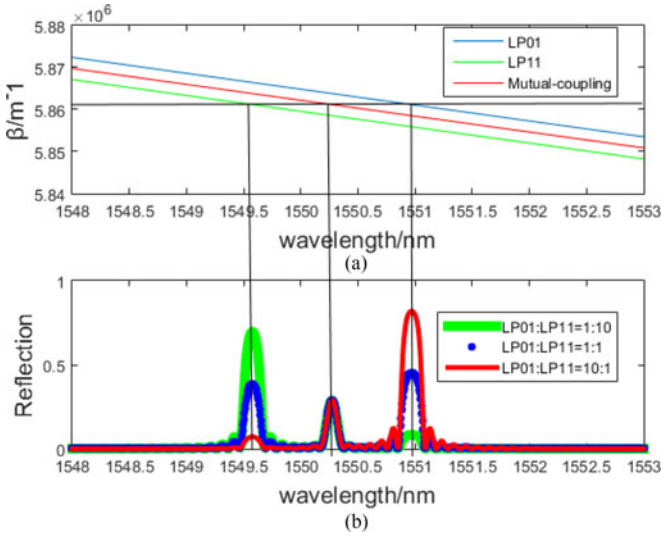

Fig. 8. Simulation of two-mode FBG with a grating period of 536 nm. (a) Optical dispersion curves and (b) reflection spectra with different mode-ratio: Blue, LP01:LP11 = 1:1; Red, LP01:LP11 = 10:1; Green, LP01:LP11 = 1:10.

3.2 Reflection Spectra of Step Index Two-Mode FBG

The mode coupling intensity inside the two-mode FBG can be described by following overlap integral:

$$K_{kj}(z) = \frac{\omega}{4} \iint_{core} \Delta\varepsilon(x, y, z)\, e_k(x, y)\, e_j(x, y) dx dy \tag{1}$$

where $e_k(x, y)$ and $e_j(x, y)$ are the normalized electric field of mode k and mode j over the fiber core cross-section. The FBG resonance wavelength is decided by the phase matching condition:$\beta_k - \beta_j = 2\pi/\Lambda$, where β_k, β_j and Λ are the propagation constant of mode k, and mode j, and period of the grating, respectively. For self-coupling, the phase matching condition can be simplified as $\lambda_B = 2n_{\text{eff}}\Lambda$ (λ_B and n_{eff} are the resonance wavelength and effective refractive index, respectively), the simplified formula for two-mode FBG is $\lambda_B = (n_{eff1} + n_{eff2})\Lambda$ (n_{eff1} for LP01 and n_{eff2} for LP11 mode)

Fig. 8(a) shows the simulated fiber dispersion curve, and Fig. 8(b) shows the reflection spectra with different mode-ratios (the mode intensity ratio between LP01 mode and LP11 mode) in a step index two-mode FBG. Three peak wavelengths represent the self-coupling and mutual-coupling between the LP01 and LP11 modes. The number of reflection peaks is decided by the mode-ratio, and the self-coupling is enhanced by increasing mode intensity contrast between LP01 and LP11 mode.

4. Conclusion

In conclusion, we have demonstrated, for the first time to our best knowledge, a SLM injection-locked fiber ring laser generating CVB near a wavelength of 1551.4 nm with a 3 dB bandwidth of < 0.01 nm and a signal-to-background ratio of > 60 dB. A step index two-mode FBG is used as the intra-cavity high-order mode selector. Our simulation and experimental results indicate high-order modes can be effectively suppressed through decreasing bent radius. Compared to the passive method without using an injection locked fiber ring cavity, our proposed method has the advantage of obtaining higher CVB purity, higher power, higher SNR, and narrower bandwidth. We anticipate this novel all-fiber CW SLM CVB laser will find potential applications in areas such as optical sensing, manipulation, and laser micro-and-nanofabrication.

References

[1] R. S. R. Ribeiro, O. Soppera, A. G. Oliva, A. Guerreiro, and P. A. Jorge, "New trends on optical fiber tweezers," *J. Lightw. Technol.*, vol. 33, no. 16, pp. 3394–3405, Aug. 2015.

[2] N. F. Chiu and W. C. Lee, "Constructing a novel asymmetric dielectric structure toward the realization of high-performance surface plasmon resonance biosensors," *IEEE Sensors J.*, vol. 13, no. 9, pp. 3483–3489, Sep. 2013.

[3] S. Ramachandran and P. Kristensen, "Optical vortices in fiber," *Nanophotonics*, vol. 2, pp. 455–474, 2016.

[4] J. Wang, "Advances in communications using optical vortices," *Photon. Res.*, vol. 4, no. 5, pp. B14–B28, 2016.

[5] Q. Zhan, "Cylindrical vector beams: From mathematical concepts to applications," *Adv. Opt. Photon.*, vol. 1, no. 1, pp. 1–57, 2009.

[6] R. Zhou, J. W. Haus, P. E. Powers, and Q. Zhan, "Vectorial fiber laser using intracavity axial birefringence," *Opt. Exp.*, vol. 18, no. 10, pp. 10839–10847, 2010.

[7] S. Ngcobo, I. Litvin, L. Burger, and A. Forbes, "A digital laser for on-demand laser modes," *Nature Commun.*, vol. 4, 2013, Art. no. 2289.

[8] Z. Bomzon, G. Biener, V. Klerner, and E. Hasman, "Radially and azimuthally polarized beams generated by space-variant dielectric subwavelength gratings," *Opt. Lett.*, vol. 27, no. 5, pp. 285–287, 2002.

[9] K. Yan and J. Lin, "Bi_2Te_3 based passively Q-switched fiber laser with cylindrical vector beam emission," *Appl. Opt.*, vol. 55, no. 11, pp. 3026–3029, 2016.

[10] B. Sun and A. T. Wang, "Mode-locked all-fiber laser producing radially polarized rectangular pulses," *Opt. Lett.*, vol. 40, no. 8, pp. 1691–1694, 2015.

[11] Y. Zhou *et al.*, "Actively mode-locked all fiber laser with cylindrical vector beam output," *Opt. Lett.*, vol. 41, no. 3, pp. 548–550, 2016.

[12] B. Sun *et al.*, "Transverse mode switchable fiber laser through wavelength tuning," *Opt. Lett.*, vol. 38, no. 5, pp. 667–669, 2013.

[13] B. Sun *et al.*, "Low threshold single wavelength all fiber laser generating cylindrical vector beam using a few mode fiber Bragg grating," *Opt. Lett.*, vol. 37, no. 4, pp. 464–466, 2012.

[14] S. Ramachandran, P. Kristensen, and M. F. Yan, "Generation and propagation of radially polarized beams in optical fibers," *Opt. Lett.*, vol. 34, no. 16, pp. 2525–2527, 2009.

[15] T. Grosjean, "An all-fiber device for generating radially and other polarized light beams," *Opt. Commun.*, vol. 203, no. 1, pp. 1–5, 2002.

[16] G. Volpe and D. Petrov, "Generation of cylindrical vector beams with few-mode fibers excited by Laguerre Gaussian beams," *Opt. Commun.*, vol. 237, no. 89, pp. 89–95, 2004.

[17] X. Liu, Y. Cui, D. Han, X. Yao, and Z. Sun, "Distributed ultrafast fibre laser," *Sci. Rep.*, vol. 5, 2015, Art. no. 9101.

[18] X. Liu and Y. Cui, "Flexible pulse-controlled fiber laser," *Sci. Rep.*, vol. 5, 2015, Art. no. 9399.

[19] X. X. Yang, L. Zhan, and Y. X. Xia, "High-power single-longitudinal-mode fiber laser employing two Sagnac loop filters," *Opt. Eng.*, vol. 47, no. 6, pp. 065001-1—065001-3, 2008.